APS physics

CHORUS

This is the accepted manuscript made available via CHORUS. The article has been published as:

Optical Coherence in Atomic-Monolayer Transition-Metal Dichalcogenides Limited by Electron-Phonon Interactions

P. Dey, J. Paul, Z. Wang, C. E. Stevens, C. Liu, A. H. Romero, J. Shan, D. J. Hilton, and D. Karaiskaj

Phys. Rev. Lett. **116**, 127402 — Published 25 March 2016

DOI: 10.1103/PhysRevLett.116.127402

Optical coherence in atomic monolayer transition metal dichalcogenides limited by electron-phonon interactions

P. Dey,[1] J. Paul,[1] Z. Wang,[2] C. E. Stevens,[1] C. Liu,[1] A. H. Romero,[3] J. Shan,[2] D. J. Hilton,[4] and D. Karaiskaj[1,*]

[1] *Department of physics, University of South Florida, 4202 East Fowler Ave., Tampa, Florida 33620*
[2] *Department of Physics, Pennsylvania State University, University Park, PA 16802, USA*
[3] *Physics Department, West Virginia University, Morgantown, WV, 26506-6315, USA*
[4] *Department of Physics, University of Alabama at Birmingham, Birmingham, Alabama 35294, USA*

We systematically investigate the excitonic dephasing of three representative transition metal dichalcogenides, namely MoS_2, $MoSe_2$ and WSe_2 atomic monolayer thick and bulk crystals, in order to gain proper understanding of the factors that determine the optical coherence in these materials. Coherent nonlinear optical spectroscopy, temperature dependent absorption combined with theoretical calculations of the phonon spectra, indicate electron-phonon interactions to be the limiting factor. Surprisingly, the excitonic dephasing differs only slightly between atomic monolayers and high quality bulk crystals, which indicates that material imperfections are not the limiting factor in atomically thin monolayer samples. The temperature dependence of the electronic band gap and the excitonic linewidth combined with '*ab initio*' calculations of the phonon energies and the phonon density of state reveal strong interaction with the E' and E" phonon modes.

Transition metal dichalcogenides (TMDs) have recently received a lot of attention and have been suggested for numerous electronic and optoelectronic applications. The ability to obtain two-dimensional materials with variable band gaps has been very attractive for transistors, photodiodes, sensors [1–11], and more recently as single photon sources [12–15]. Furthermore, the preservation of the optical coherence is of importance to quantum computation devices [16, 17]. Therefore, understanding the fundamental many-body interactions and how these interactions influence the optical properties of these materials is crucially important.

As bulk materials TMDs are indirect band semiconductors with rather poor optical properties. However, when reduced to atomic monolayer they transition to direct band gap materials leading to greatly enhanced emission [1]. When photon absorption occurs electrons are excited from the valence band to the conduction band. The Coulomb interaction between the positively charged hole and the electron leads to a new quasi-particle, namely the exciton. Excitons are of importance for the optical properties of semiconductors, therefore understanding their properties, such as coherence loss or dephasing and population decay are crucial for many optoelectronic and photonic devices [18]. In direct band gap semiconductors direct excitons dominate the optical properties as compared to indirect band gap materials where indirect excitons, require momentum-conservation for emission to occur. The momentum conservation is provided by phonons, the quantized thermal vibrations of the crystal. Phonons play a crucial role in determining the optical coherence and lifetime of direct excitons through electron-phonon interactions [19].

The strength of electron-phonon interactions often determines the optical properties of materials and can be a limiting factor for many applications. While the inhomogeneous linewidth of excitons is determined by material imperfections and can be reduced by improving the material quality, the homogeneous linewidth is often limited by the fundamental interactions taking place, which place limitations on the material system. In the present study we systematically investigate three representative TMDs, namely MoS_2, $MoSe_2$ and WSe_2 as monoatomic thick layer and bulk crystals, in order to understand the fundametal interactions taking place and how they limit the excitonic homogeneous linewidth. The excitonic coherence is a direct measure of the homogeneous linewidth, therefore processes leading to dephasing can be the limiting factor [21]. In order to obtain a complete understanding of the dephasing mechanism, we combine several techniques with state-of-the-art calculation of the phonon spectra.

We measure the dephasing time for atomic monolayer MoS_2, WSe_2 and $MoSe_2$. The excitonic dephasing is very rapid leading to fairly large homogeneous excitonic linewidths, but dephasing time increases slightly from MoS_2 in WSe_2 and further in $MoSe_2$. Furthermore, we were able to measure the excitonic dephasing in high quality bulk WSe_2 crystals, which is only slightly longer as compared to the monolayer. This surprising result indicates that any sample imperfections due to exfoliating down to atomic monolayer or due to the choice of the substrate are not the limiting factors. Therefore, the limiting mechanism is likely to be intrinsic. The excitation density and temperature dependence of the dephasing time reveal a residual homogeneous excitonic linewidth for MoS_2 of $\sim$4.5 meV. These measurements indicate that temperature i.e., electron-phonon interactions set the limit on the homogeneous linewidth.

We further proceed by measuring the energy shift and broadening of the direct excitons in bulk MoS_2, WSe_2 and $MoSe_2$ crystals and obtain the dominating phonon energies. *'Ab initio'* calculations of the phonon energies and density of states pinpoint to the E' and E" phonon

* karaiskaj@usf.edu

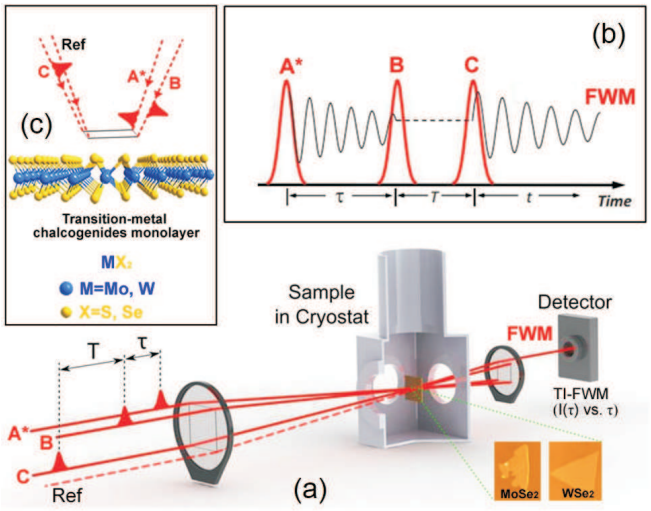

FIG. 1. (a) The four phase-stabilized linearly polarized beams obtained from the multi-dimensional optical nonlinear spectrometer (MONSTR) instrument described in Ref. 20 are focused on the sample, which is held in the cryostat at 5 K. The FWM signal can be measured as a function of the time delays τ and T using a detector, which integrates over the time delay t. (b) The sequence of the laser pulses used in the experiments, where A* corresponds to the phase conjugated pulse. The time delay τ corresponds to the time between the pulses A* and B, T is the time delay between the pulses B and C, and t is the evolution of the echo in 'real time'. (c) Crystal structure of atomic monolayer TMDs. In bulk TMDs the unit cell extends over two layers bound through Van der Waals interaction along the c-axis. The laser excitation shown is perpendicular to the covalently bound layers or parallel to the c-axis.

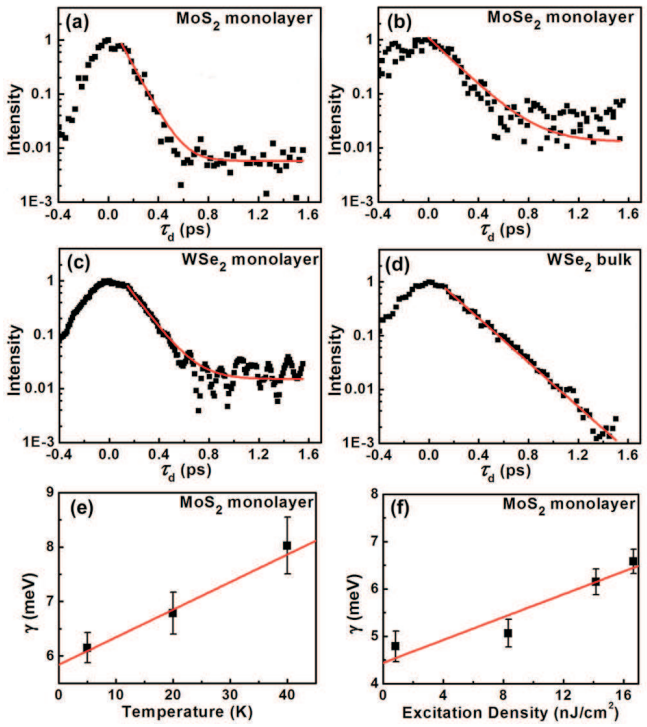

FIG. 2. (a-c) Time-integrated FWM of atomic monolayers (a) MoS_2 (b) $MoSe_2$ and (c) WSe_2. (d) Time-integrated FWM of the direct excitons in bulk WSe_2. The black symbols are the experimental data whereas the red line is the single exponential fit.(e) Temperature dependence of the homogeneous linewidth for atomic monolayer MoS_2. Squares are the measured values whereas the red line is the linear fit. (f) Excitation density dependence of the homogeneous linewidth for atomic monolayer MoS_2. Circles are the measured values whereas the red line is the linear fit.

modes. These phonon modes interact strongly with the electronic states and are thought to cause the efficient excitonic dephasing observed. Furthermore, calculations of the phonon density of states (DOS) of atomic monolayers lead to very similar, almost undistinguishable results from the bulk crystals, which supports the very similar dephasing rate of excitons observed in bulk and atomic monolayer samples.

The four-wave mixing (FWM) technique can measure the excitonic dephasing directly. The setup used in the present study is shown in Fig. 1. Three consecutive laser pulses of ∼130 fs duration are used to excite the A excitons resonantly and are separated by two time delays τ and T. By maintaining the time delay T fixed and scanning τ in a time-integrated FWM experiment the dephasing time T_2 can be measured. The dephasing time T_2 is related to the homogeneous linewidth by a simple relationship $\gamma = 2\hbar/T_2$. The linear absorption spectra in these materials are dominated by inhomogeneous broadening due to defects and unintentional impurities which conceals the homogeneous linewidths.

We start by discussing the time-integrated FWM measurements shown in Fig. 2. The dephasing time T_2 provides the homogeneous linewidth and was measured for atomic monolayers of MoS_2, WSe_2 and $MoSe_2$ to be 200 fs (∼6.58 meV), 279 fs (∼4.72 meV), and 394 fs (∼3.34 meV) respectively, showing a rapid decay for all the materials. Furthermore, we were able to measure the dephasing of direct excitons in bulk WSe_2 shown in Fig. 2 (d) despite of the bulk material being an indirect band gap semiconductor. The dephasing time of 422 fs (∼3.12 meV) increased little in the bulk material as compared to the atomic monolayer WSe_2. The atomic monolayer samples are exfoliated from bulk samples and are suspended on quartz substrates. Defects introduced during the exfoliation process and the effect of the substrate could perhaps change the excitonic properties of the atomic monolayer samples. In bulk crystals direct excitons are thought to have a lower binding energy than monolayers [22–26] and most excitons are well shielded from the substrate. The two-dimensional atomic layers deeper under the surface layers should not have sustained any mechanical damage through exfoliation. However, the similar dephasing rate observed in bulk and atomic monolayer WSe_2 suggest that it is caused by underlying intrinsic effects which are shared by both samples.

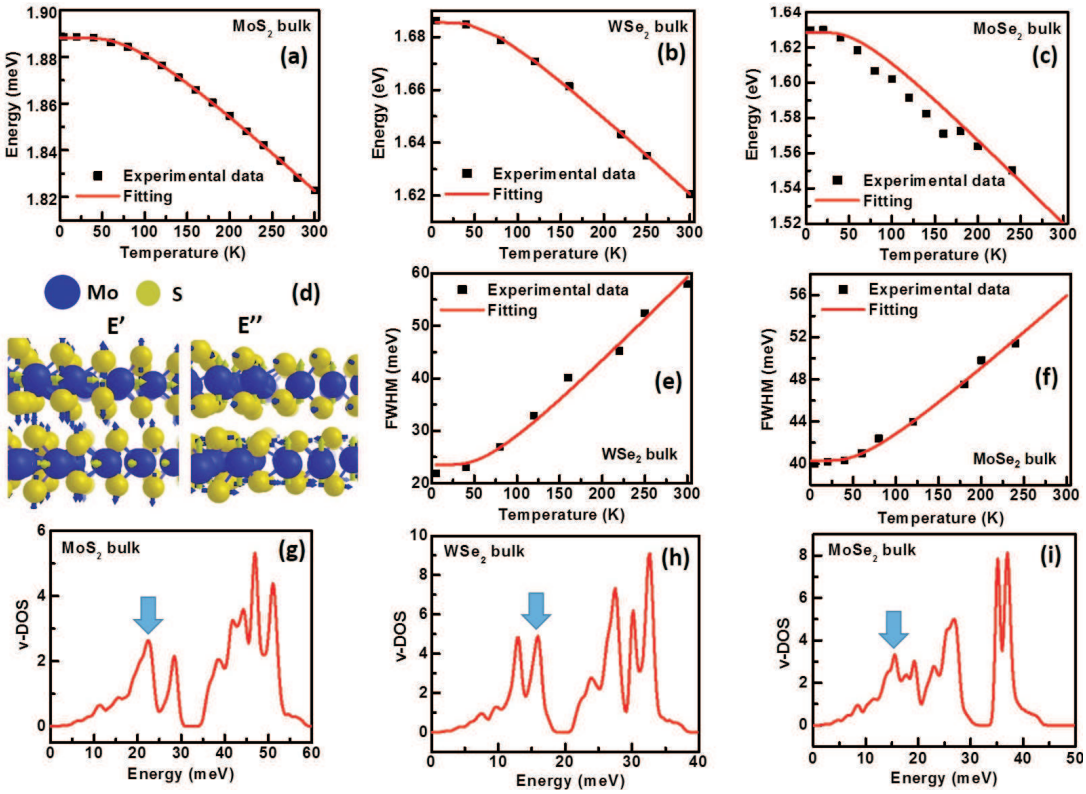

FIG. 3. (a) Temperature dependence of the electronic band gap for bulk (a) MoS_2, (b) WSe_2, and (c) $MoSe_2$. The black squares are the experimental values whereas the red line is the fitting using equation 1. Temperature broadening of the direct excitons in bulk (e) $MoSe_2$ and (f) WSe_2. The black squares are the experimental values whereas the red line is the fitting using equation 2 (d) Schematic of the E' and E" phonon modes which are a result of the fittings. Calculated phonon density of states for bulk (g) MoS_2, (h) $MoSe_2$, and (i) WSe_2. The blue arrows indicate the phonon energies used in the fittings.

By maintaining the time delay $\tau = 0$ ps fixed and scanning the time delay T the FWM intensity decays according to the population time T_1. The population decay time of excitons in the WSe_2 crystal was measured to decay very rapidly at ∼3 ps. The rapid decay of the population is expected due to the large excitonic oscillator strength obtained from the absorption measurements. The rapid initial decay is followed by much longer decay time of ∼100 ps likely due to trapped excitons at impurities or defects. The temperature dependence of the homogeneous linewidth for atomic monolayer MoS_2 is shown in Fig. 2 (e) and the homogeneous linewidth γ increases very rapidly with temperature. At temperatures higher than 40 K it exceeds our ability to measure it. The scattering rate of excitons with acoustic phonons at low temperature is described by a linear relationship $\gamma = \gamma^* + aT$, where γ^* is the temperature independent broadening originating from other sources. The linear fit leads to an acoustic phonon scattering coefficient a ∼ 45 μeV/K, which is large and indicates strong electron-phonon interactions. Furthermore, the excitation density dependence of the homogeneous linewidth γ is shown in Fig. 2 (f) and exhibits some excitation induced dephasing [27]. However, at the limit of 'zero' excitation power the residual homogeneous linewidth independent of excitation density is ∼4.5 meV.

In order to obtain a quantitative understanding of the electron-phonon interactions in TMDs we carefully measure the energy shift of the electronic band gap with temperature. Temperature dependent absorption spectra of the excitons provide the energy shift of the band gap with temperature and also the temperature broadening of the excitonic resonance. These effects are in large part a result of electron-phonon interactions [28–32]. The energy shift of the exciton resonance with temperature for bulk MoS_2, $MoSe_2$, and WSe_2 obtained from the absorption spectra are shown in Fig. 3 (a-c), where the black squares are the experimental data and the red line is the theoretical fit. The fitting procedure was performed using the approximate model introduced in Ref. 32,

$$E_g = E_0 - E_1 \left[2(\exp\left(\frac{\Theta}{kT}\right) - 1)^{-1} + 1 \right] \qquad (1)$$

where E_0 and E_1 are fitting parameters, whereas Θ is either a dominant phonon or an average phonon energy. The absorption spectra of the excitons in TMDs at low temperature are predominantly inhomogeneously broadened. The inhomogeneous broadening is due not only to intrinsic material imperfections but in bulk samples also

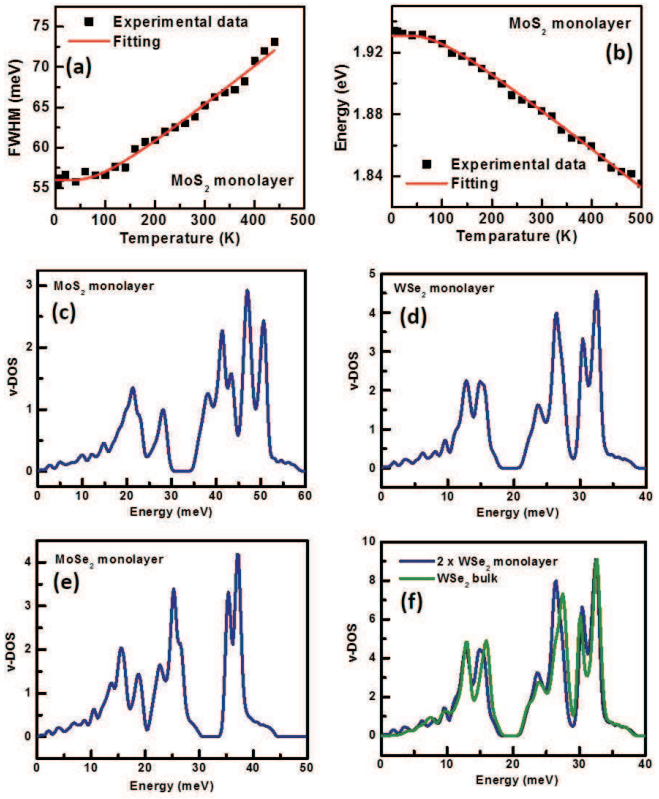

FIG. 4. (a) Temperature broadening of the direct excitons for an atomic monolayer MoS_2. (b) Temperature dependence of the electronic band gap for an atomic monolayer MoS_2. Calculated phonon density of states for atomic monolayer (c) MoS_2, (d) $MoSe_2$, and (e) WSe_2. (f) Comparison of the calculated phonon density of states for atomic monolayer and bulk WSe_2.

due to varying thickness as result of the sample preparation. However, as the temperature rises, the phonon scattering leads to observable broadening since the lineshapes are a convolution of homogeneous and inhomogeneous contributions. The linewidths of the exciton absorption spectra as a function of temperature for $MoSe_2$ and WSe_2 are plotted in Fig. 3 (e-f), were the black squares are the experimental data, whereas the red line is the theoretical fit. The theoretical fit was performed according to

$$\gamma = \gamma_I + \frac{b}{\exp(\Theta/kT) - 1} \qquad (2)$$

where γ_I is the temperature independent inhomogeneous broadening. Both the energy shift and broadening of the excitonic resonance can be fitted simultaneously by using a phonon energy $\Theta = 22.1$ meV, 16.3 meV and 15.5 meV for MoS_2, WSe_2, and $MoSe_2$, respectively.

In order to be able to identify the phonon energies and gain a deeper understanding of the dephasing mechanism we performed state-of-the-art *'ab initio'* calculations of the phonon spectra and phonon DOS for bulk and atomic monolayer TMDs [33–43]. The phonon DOS for MoS_2, WSe_2, and $MoSe_2$ are shown in Fig. 3 (g-i), where the blue arrows marks the energies of the Θ phonons obtain from the fitting of the experimental data. Clear peaks in the phonon DOS can be observed at these energies. The calculations also reveal two phonon modes at these energies corresponding to the E' and E" representation. The calculated phonon energies are 23.3 (E') meV and 23.5 (E") meV for MoS_2, 12.6 (E') and 15.8 (E") for WSe_2, and 15.8 meV (E') and 17.7 meV (E") for $MoSe_2$ and a schematic of the vibration for both modes is shown in Fig. 3 (d). These energies are very close to the observed phonon energies. However, the two modes are energetically very close which makes it difficult to distinguish them experimentally.

We further proceed by examining the temperature dependence of the excitonic resonance and the electronic band gap for atomic monolayer MoS_2. The experimental data together with the fits are shown in Fig. 4 (a) and (b), respectively. The same phonon energy has been used in the fitting procedure as used for the bulk MoS_2 sample, leading to very good agreement with the experimental data. The calculated phonon DOS for atomic monolayer MoS_2, WSe_2, and $MoSe_2$ is shown in Fig. 4 (c-e). The phonon DOS show very similar structure as compared to bulk crystals in particular around the E' and E" phonon modes. In Fig. 4 (f) the phonon DOS is shown for both, atomic monolayer and bulk WSe_2 for comparison. There are very minimal difference between the two spectra, indicating that the electron-phonon interactions are expected to be very similar. This is well in agreement with the comparable exciton dephasing rates observed atomic monolayer and bulk. The increased quantum confinement in atomic monolayer TMDs would lead to somewhat stronger exciton scattering by phonons and as a result to even faster dephasing, which is in agreement with the experimental observation.

In conclusion, we provide a detailed description of the dephasing mechanism of free direct excitons in atomic monolayer TMDs. The dephsing time in atomic monolayer samples does not differ significantly from bulk crystals, despite the different confinement and excitonic binding energies. The temperature dependence and excitation density dependence of the dephasing in atomic monolayers indicate that the electron-phonon interactions determine the rapid dephasing, and as a result, the large residual homogeneous linewidths in this material system. We systematically examine the electron-phonon interactions in bulk TMDs by measuring the energy shift on the electronic band gap and broadening of the direct excitons with temperature. Fitting using known models provide the phonon energies of interest. State-of-the-art calculations of the phonon energies and phonon DOS determined these phonon energies as the E' and E" phonon modes, which are thought to be responsible for the rapid dephasing in TMDs. The calculated phonon DOS in bulk and atomic monolayer are strikingly similar, which is well in agreement with the similar dephasing rates observed

in both material systems.

ACKNOWLEDGMENTS

The research at USF, Penn. State, and UAB is supported by the U.S. Department of Energy, Office of Basic Energy Sciences, Division of Materials Sciences and Engineering under Award DE-SC0012635. AHR acknowledges the support from the Extreme Science and Engineering Discovery Environment (XSEDE), which is supported by National Science Foundation Grant No. ACI-1053575, the support of NSF under project 1434897 and the Donors of the American Chemical Society Petroleum Research Fund for partial support of this research under contract 54075-ND10.

[1] K. F. Mak, C. Lee, J. Hone, J. Shan, and T. F. Heinz, Phys. Rev. Lett. **105**, 136805 (2010).
[2] K. F. Mak, K. He, J. Shan, and T. F. Heinz, Nature Nanotechnology **7**, 494 (2012).
[3] H. Zeng, J. Dai, W. Yao, D. Xiao, and X. Cui, Nature Nanotechnology **7**, 490 (2012).
[4] T. Cao, G. Wang, W. Han, H. Ye, C. Zhu, J. Shi, Q. Niu, P. Tan, E. Wang, B. Liu, and J. Feng, Nature Communications **3**, 887 (2012).
[5] K. F. Mak, K. He, C. Lee, G. Hyoung, J. Hone, T. F. Heinz, and J. Shan, Nature Materials **13**, 207 (2013).
[6] A. M. Jones, H. Yu, N. J. Ghimire, S. Wu, G. Aivazian, J. S. Ross, B. Zhao, J. Yan, D. G. Mandrus, D. Xiao, W. Yao, and X. Xu, Nature Nanotechnology **8**, 634 (2013).
[7] J. A. Schuller, S. Karaveli, T. Schiros, K. He, S. Yang, I. Kymissis, J. Shan, and R. Zia, Nature Nanotechnology **8**, 271 (2013).
[8] S. Wu, J. S. Ross, G.-B. Liu, G. Aivazian, A. Jones, Z. Fei, W. Zhu, D. Xiao, W. Yao, D. Cobden, and X. Xu, Nature physics **9**, 149 (2013).
[9] T. Georgiou, R. Jalil, B. D. Belle, L. Britnell, R. V. Gorbachev, S. V. Morozov, Y.-J. Kim, A. Gholinia, S. J. Haigh, O. Makarovsky, L. Eaves, L. A. Ponomarenko, A. K. Geim, K. S. Novoselov, and A. Mishchenko, Nature Nanotechnology **8**, 100 (2013).
[10] K. F. Mak, K. L. McGill, J. Park, and P. L. McEuen, Science **344**, 1489 (2014).
[11] C. Poellmann, P. Steinleitner, U. Leierseder, P. Nagler, G. Plechinger, M. Porer, R. Bratschitsch, C. Schller, T. Korn, and R. Huber, Nature Mat. **14**, 889 (2015).
[12] A. Srivastava, M. Sidler, A. V. Allain, D. S. Lembke, A. Kis, and A. Imamoglu, Nature Nanotechnology **10**, 491 (2015).
[13] Y.-M. He, G. Clark, J. R. Schaibley, Y. He, M.-C. Chen, Y.-J. Wei, X. Ding, Q. Zhang, W. Yao, X. Xu, C.-Y. Lu, and J.-W. Pan, Nature Nanotechnology **10**, 497 (2015).
[14] M. Koperski, K. Nogajewski, A. Arora, V. Cherkez, P. Mallet, J.-Y. Veuillen, J. Marcus, P. Kossacki, and M. Potemski, Nature Nanotechnology **10**, 503 (2015).
[15] C. Chakraborty, L. Kinnischtzke, K. M. Goodfellow, and R. B. A. N. Vamivakas, Nature Nanotechnology **10**, 507 (2015).
[16] L. C. Bassett, F. J. Heremans, D. J. Christle, C. G. Yale, G. Burkard, B. B. Buckley, and D. D. Awschalom, Science **345**, 1333 (2014).
[17] G. Moody, C. K. Dass, K. Hao, C.-H. Chen, L.-J. Li, A. Singh, K. Tran, G. Clark, X. Xu, G. Berghuser, E. Malic, A. Knorr, and X. Li, Nat. Commun. **6**, 1038 (2015).
[18] H. Haug and S. W. Koch, *Quantum Theory of Optical and Electronic Properties of Semiconductors* (World Scientific, 2009).
[19] P. Y. Yu and M. Cardona, *Fundamentals of Semiconductors: Physics and Materials Properties* (Springer-Verlag, 2010).
[20] P. Dey, J. Paul, J. Bylsma, S. Deminico, and D. Karaiskaj, Review of Scientific Instruments **84**, 023107 (2013).
[21] S. T. Cundiff, Opt. Express **16**, 4639 (2008).
[22] D. Y. Qiu, F. H. da Jornada, and S. G. Louie, Phys. Rev. Lett. **111**, 216805 (2013).
[23] K. He, N. Kumar, L. Zhao, Z. Wang, K. F. Mak, H. Zhao, and J. Shan, Phys. Rev. Lett. **113**, 026803 (2014).
[24] E. Fortin and F. Raga, Phys. Rev. B **11**, 905 (1975).
[25] A. Anedda, E. Fortin, and F. Raga, Can. J. Phys. **57**, 368 (1979).
[26] A. Anedda and E. Fortin, J. Phys. Chem. Solids **41**, 865 (1980).
[27] J. Shah, *Ultrafast Spectroscopy of Semiconductors and Semiconductor Nanostructures* (Springer-Verlag, 1999).
[28] P. B. Allen and V. Heine, J. Phys. C: Solid State Phys. **9**, 2305 (1976).
[29] D. Olguin, M. Cardona, and A. Cantarero, Sol. Stat. Commun. **122**, 575 (2002).
[30] S. Gopalan, P. Lautenschlager, and M. Cardona, Phys. Rev. B **35**, 5577 (1987).
[31] P. Lautenschlager, P. B. Allen, and M. Cardona, Phys. Rev. B **33**, 5501 (1986).
[32] L. Viña, S. Logothetidis, and M. Cardona, Phys. Rev. B **30**, 1979 (1984).
[33] P. E. Blöchl, Phys. Rev. B **50**, 17953 (1994).
[34] G. Kresse and D. Joubert, Phys. Rev. B **59**, 1758 (1999).
[35] G. Kresse and J. Hafner, Phys. Rev. B **47**, 558 (1993).
[36] G. Kresse and J. Hafner, Phys. Rev. B **49**, 14251 (1994).
[37] G. Kresse and J. Furthmüller, Phys. Rev. B **54**, 11169 (1996).
[38] G. Kresse and J. Furthmüller, Phys. Rev. B **54**, 11169 (1996).
[39] J. P. Perdew, K. Burke, and M. Ernzerhof, Phys. Rev. Lett. **77**, 3865 (1996).
[40] M. Dion, H. Rydberg, E. Schröder, D. C. Langreth, and B. I. Lundqvist, Phys. Rev. Lett. **92**, 246401 (2004).
[41] J. Klimeš, D. R. Bowler, and A. Michaelides, J. Phys.: Cond. Matt. **22**, 022201 (2010).
[42] J. Klimeš, D. R. Bowler, and A. Michaelides, Phys. Rev. B **83**, 195131 (2011).
[43] A. Togo, F. Oba, and I. Tanaka, Phys. Rev. B **83**, 134106 (2008).